Micelle Formation of Random Copolymers of Sodium 2-(Acrylamido)-2-methylpropanesulfonate and a Nonionic Surfactant Macromonomer in Water As Studied by Fluorescence and Dynamic Light Scattering

Tetsuya Noda, Akihito Hashidzume, and Yotaro Morishima*

Department of Macromolecular Science, Graduate School of Science, Osaka University, Toyonaka, Osaka 560-0043, Japan

Received October 5, 1999; Revised Manuscript Received March 23, 2000

ABSTRACT: A polyelectrolyte-bound nonionic surfactant ($HO(CH_2CH_2O)_{25}C_{12}H_{25}$) ($C_{12}E_{25}$) system was prepared by copolymerization of sodium 2-(acrylamido)-2-methylpropanesulfonate (AMPS) and a methacrylate substituted with $HO(CH_2CH_2O)_{25}C_{12}H_{25}$ in *N*,*N*-dimethylformamide initiated by 2,2′-azobis(isobutyronitrile). The contents of the surfactant macromonomer unit (f_{DE25}) in the copolymers are in the range 10−30 mol %. Dry samples of these copolymers are soluble in water, polymer-bound surfactants undergoing micellization. The micelle formation was studied by fluorescence and quasielastic light scattering (QELS) techniques in 0.1 M NaCl aqueous solutions. Steady-state fluorescence data for pyrene probes solubilized in water in the presence of the copolymers suggest that the polymer-bound surfactants associate in both intra- and interpolymer fashions to form micelles. The interpolymer hydrophobic associations were found to commence to occur at a relatively well-defined polymer concentration (C_p), which can be regarded as an apparent "cmc" for interpolymer micelle formation. Such cmc values are 10−100 times smaller than that for discrete $C_{12}E_{25}$ molecules, the values increasing with increasing f_{DE25}. Mean aggregation numbers (N_{agg}) of the terminal dodecyl groups at an end of the $(CH_2CH_2O)_{25}$ spacer group were estimated by a time-dependent fluorescence method. N_{agg} values were found to be of the same order of that for the discrete $C_{12}E_{25}$ micelles although the values for the polymer-bound surfactant micelles are somewhat larger than that for the free micelle. The N_{agg} values were relatively constant over a significant range of C_p. QELS data indicated bimodal distributions of relaxation times with a fast and a slow relaxation mode. The slow mode component is due to polymer aggregates that include a number of micelle units formed by polymer-bound $C_{12}E_{25}$ groups. On the other hand, the fast mode component may be attributed to either a "unimeric" micelle (a micelle formed by a single polymer chain) or an "oligomeric" micelle (a micelle formed by a small number of polymer chains). Hydrodynamic radii (R_h) for the slow mode component are on the order of 60−170 nm exhibiting a tendency to increase with increasing C_p whereas those for the fast mode are 6−8 nm independent of C_p. R_h for discrete $C_{12}E_{25}$ micelle was found to be ca. 5 nm under the same conditions. On the basis of the characterization, a hypothetical micelle model was proposed where micelle units formed from polymer-bound $C_{12}E_{25}$ moieties are bridged by polymer chains yielding a micelle network structure.

Introduction

Self-association phenomena for hydrophobically modified water-soluble polymers in aqueous environments are of current scientific and technological interest because of their relevance to biological systems and also to various industrial applications.[1−11] Of particular interest is a class of amphiphilic polymers that undergo spontaneous self-organization in aqueous media mainly due to the hydrophobic associations to form various types of micelle-like nanostructures.[12−14] Hydrophobically modified polyelectrolytes are such systems that have been most extensively studied so far.[14]

In the case of hydrophobically modified polyelectrolytes, hydrophobic self-associations can occur in an intra- or interpolymer fashion competing with electrostatic repulsions within the same polymer chain or between different polymer chains, respectively. The preference of intra- or interpolymer hydrophobe association strongly depends on macromolecular architecture. Some of the structural parameters that control intra- vs interpolymer association include the type of hydrophobes, their content in the polymer, the sequence distribution of electrolyte and hydrophobic monomer units along the polymer chain, and the type of spacer between hydrophobes and the main chain.[15−18]

In the process of self-association of polymer-bound hydrophobes, the polymer chain would impose steric constraints to the hydrophobes, affecting the motional and geometrical freedom of polymer-bound hydrophobes. Therefore, the spacer between hydrophobes and the polymer backbone is an important structural factor to control self-association of polymer-bound hydrophobes.

We previously reported that the associative properties of hydrophobes linked to a polyelectrolyte via amide and ester spacer bonds are remarkably different.[14,16−26] Amide-linked hydrophobes exhibit a strong tendency for intrapolymer association whereas ester-linked hydrophobes show a propensity for interpolymer association as well as intrapolymer association. Random copolymers of sodium 2-(acrylamido)-2-methylpropanesulfonate (AMPS) with *N*-dodecylmethacrylamide (DodMAm) show a strong preference for intrapolymer self-association even in a concentrated regime, leading to the formation of unimolecular micelles.[14,16,19−27] In sharp contrast, random copolymers of AMPS and dodecyl methacrylate (DMA) exhibit a tendency for interpolymer association, leading to the formation of multipolymer micelles.[18] Furthermore, there is a great difference in the solubility in water between the AMPS copolymers having amide- and ester-linked hydrophobes. AMPS−DodMAm copoly-

10.1021/ma991680x CCC: $19.00
Published on Web 04/29/2000

Chart 1. Chemical Structure of Copolymers Studied

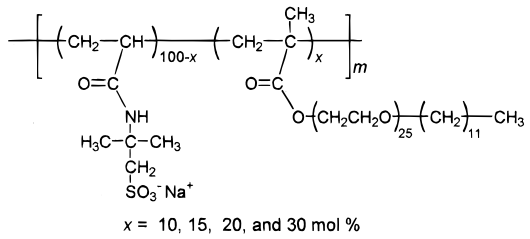

x = 10, 15, 20, and 30 mol %

mers are soluble in water up to about 60 mol % hydrophobe content,[27] whereas AMPS−DMA copolymers were soluble in water only when the hydrophobe content is as low as 15 mol %.

Moreover, interpolymer association occurs more favorably when the length of the spacer bond is increased.[17] Random copolymers of AMPS and cholesteryl 6-methacryloyloxyhexanoate show a strong tendency for interpolymer association, compared to random copolymers of AMPS and cholesteryl methacrylate. In the former copolymer, cholesterol is linked to the main chain via a $(CH_2)_5$ spacer between two ester bonds whereas in the latter copolymer, cholesterol is attached to the main chain via an ester bond. The $(CH_2)_5$ spacer-linked cholesterol moieties form intermolecularly bridged "flower-like" micelles even if the cholesterol content in the copolymer is <5 mol %.[17]

The objective of the present study is to elucidate association properties of an amphiphilic polyelectrolyte carrying hydrophobes linked via a long, flexible hydrophilic spacer where hydrophobes are much less restricted by the polymer backbone. Polymers synthesized in this study are random copolymers of AMPS and a methacrylate substituted with poly(ethylene oxide) (PEO) mono-*n*-dodecyl ether of the number-average degree of polymerization (i) = 25 for the $(CH_2CH_2O)_i$ spacer (DE25MA) (Chart 1). We will report on the association behavior of the AMPS−DE25MA copolymers with the macromonomer content (f_{DE25}) ranging from 10 to 30 mol % in 0.1 M NaCl aqueous solutions. These polymers can be visualized as an macromolecular system where a large number of surfactant fragments are linked to the same backbone. Fluorescence techniques, using pyrene as a probe, and quasielastic light scattering (QELS) techniques were employed to monitor hydrophobe associations to characterize the self-association behavior. We observed that a nonionic surfactant, PEO mono-*n*-dodecyl ether of a number-average degree of polymerization of 25 ($C_{12}E_{25}$), formed micelles with a mean aggregation number (N_{agg}) of dodecyl groups of ca. 40 and an apparent hydrodynamic radius (R_h) of ca. 5 nm in 0.1 M NaCl aqueous solutions. Our attention was particularly focused on whether polyelectrolyte-bound $C_{12}E_{25}$ moieties can form micelles similar to those formed by discrete $C_{12}E_{25}$ molecules and, if so, whether such polymer-bound micelles are formed by intra- or interpolymer association or both. On the basis of experimental results, we proposed a hypothetical model for the hydrophobe associations in AMPS−DE25MA copolymers with varying f_{DE25}.

Experimental Section

Materials. Poly(ethylene oxide) mono-*n*-dodecyl ether of a number-average degree of polymerization of 25 ($C_{12}E_{25}$) and 2-(acrylamido)-2-methylpropanesulfonic acid (AMPS), both purchased from Wako Pure Chemical Co., were used without further purification. Methacryloyl chloride (purchased from Wako Pure Chemical Co.), benzene, and *N*,*N*-dimethylformamide (DMF) were distilled under reduced pressure over calcium hydride. 2,2′-Azobis(isobutyronitrile) (AIBN) was recrystallized from ethanol. Pyrene was recrystallized twice from ethanol. Water was purified with a Millipore Milli-Q system. Other reagents were used as received.

Macromonomer (DE25MA). Methacrylate end-capped macromonomer (DE25MA) was prepared as follows: Methacryloyl chloride (1.47 mL, 15.0 mmol) was added to a solution of $C_{12}E_{25}$ (6.94 g, 5.0 mmol) and triethylamine (2.09 mL, 15.0 mmol) in benzene at 0 °C over a period of 15 min with stirring under an Ar atmosphere, followed by stirring for an additional 24 h under the same conditions. After removing triethylamine HCl salt by filtration, the solvent was evaporated. The macromonomer, obtained as a jellylike solid in a yield of 92.9% (6.49 g), was characterized by ^{1}H NMR to be ca. 98% pure with ca. 2% unreacted $C_{12}E_{25}$ remaining.

Polymers. The copolymers of AMPS and DE25MA were prepared by free radical copolymerization in the presence of AIBN in DMF. A representative procedure for the copolymerization is as follows: A known amount of AMPS was neutralized by equinormal of Na_2CO_3 in DMF, and predetermined amounts of DE25MA and AIBN were added to this solution. The mixture of the monomers and the initiator was placed in a glass ampule and outgassed on a high-vacuum line by six freeze−pump−thaw cycles. The ampule was then sealed under high vacuum. Polymerization was carried out at 60 °C for 21 h. The polymerization mixture was poured into a large excess of diethyl ether to precipitate the resulting polymer. The polymer was purified by reprecipitation from methanol into a large excess of diethyl ether three times and then dissolved in pure water. The aqueous solution was dialyzed against pure water for a week using a cellulose tube (Viskase Sales Co., pore size 36/32, corresponding to an MW cutoff 12 000−14 000), and the polymer was recovered by a freeze-drying technique. The composition of the copolymer was determined by ^{1}H NMR spectroscopy.

Measurements. a. NMR. The ^{1}H NMR spectrum of DE25MA was measured with a JEOL GSX-400 NMR spectrometer in $CDCl_3$ at 30 °C. ^{1}H NMR spectra of the polymers were measured using D_2O as a solvent at 60 °C. Chemical shifts were determined by using TMS as an internal standard.

b. Gel Permeation Chromatography (GPC). GPC measurements were performed at 40 °C with a JASCO GPC-900 equipped with an Asahipak GF-7M HQ column (Shodex) in combination with JASCO UV-975 and RI-930 detectors. A 0.1 M $LiClO_4$ methanol solution was used as an eluent. Molecular weights of polymers were calibrated by standard poly(ethylene glycol) (Scientific Polymer Products, Inc.). For all the measurements, the elution rates were fixed to 1.0 mL/min.

c. Absorption Spectra. Absorption spectra were recorded on a JASCO V-550 spectrophotometer using a 1.0 cm path length quartz cell. The concentrations of pyrene solubilized in the polymer phase were calculated from the absorbances at 338 nm using $\epsilon_{338} = 37\,000\ M^{-1}\ cm^{-1}$ as the molar extinction coefficient.[28]

d. Fluorescence. *(1) Steady-State Fluorescence Measurements.* Steady-state fluorescence spectra were recorded on a Hitachi F-4500 fluorescence spectrophotometer. Emission spectra of pyrene were measured with excitation at 337 nm at room temperature. Excitation spectra were monitored at 372 nm. The slit widths for both the excitation and emission sides were kept at 2.5 nm during measurements. Sample solutions were prepared by dissolving a known amount of polymer in an aqueous pyrene solution of a known concentration, and the solutions were allowed to stand for 1 day for equilibration. Aqueous pyrene solutions of given concentrations were prepared by diluting pyrene-saturated water.[17]

For the determination of the critical micelle concentration (cmc) of the polymers, excitation spectra of pyrene were measured at varying concentrations of pyrene and the polymers, as reported by Wilhelm et al.[29]

(2) Time-Resolved Fluorescence Measurements. Fluorescence decay data were collected on a HORIBA NAES 550 system equipped with a flash lamp filled with hydrogen. Sample

solutions containing pyrene as a fluorescence probe were excited at 337 nm, and pyrene fluorescence was monitored around 400 nm with a band-pass filter (Toshiba KL-40) and a cutoff filter (Toshiba L-38) placed between the sample and detector. Sample solutions were prepared as described above and purged with Ar for about 30 min prior to measurement. Measurements were performed with a pyrene concentration of 1×10^{-7} M. The observed decay is a convolution of the sample decay function and the instrumental response function. Fluorescence decay data were fitted to a single- or double-exponential function. For criteria for the goodness of the fit, χ^2 and the weighted residuals were used.

The aggregation number (N_{agg}) of the polymer hydrophobes was determined by using pyrene as a fluorescence probe. Pyrene molecules were solubilized in the polymer micelles at high concentrations such that excimer was formed within the micelles. Sample solutions were prepared by pouring a small amount of a concentrated pyrene solution in acetone into aqueous solutions of the polymer. All sample solutions were filtered with a 0.2 μm membrane filter prior to measurement. The determination of N_{agg} is based on the Infelta−Tachiya equation for quenching in monodisperse micelles.[30,31] In the present study, the quenching of pyrene monomer fluorescence, arising from excimer formation, was used to determine N_{agg}. Fluorescence decay data were fitted to the following equation, assuming the distributions of fluorescence probe molecules over the micelles obey a Poisson distribution.

$$\ln[I(t)/I(0)] = A_3[\exp(-A_4 t) - 1] - A_2 t \quad (1)$$

$$A_2 = k_0 + n_Q k_Q k^-/(k_Q + k^-) \quad (2a)$$

$$A_3 = n_Q k_Q{}^2/(k_Q + k^-)^2 \quad (2b)$$

$$A_4 = k_Q + k^- \quad (2c)$$

Here, $I(t)$ and $I(0)$ are the fluorescence intensities at time t and 0 following pulse excitation, respectively, k_Q is the pseudo-first-order rate constant for quenching of the excited probe, k_0 ($=\tau_0^{-1}$) is the fluorescence decay rate constant for pyrene inside the micelle without excimer formation, n_Q is the average number of quenchers dissolved into a micelle, and k^- is the first-order rate constant for exit of pyrene molecules from a micelle. n_Q can be expressed as $[Q]_m/[M]$, where $[Q]_m$ is the molar concentration of quencher inside micelle and [M] is the molar concentration of micelles. Because the quenching of pyrene monomer fluorescence is due to the excimer formation of pyrene in this study, $[Q]_m$ corresponds to the concentration of pyrene. The $[Q]_m/[M]$ ratio ($=n_Q$) was determined from the best fit. N_{agg} is calculated from thus determined $[Q]_m/[M]$ ratio. The details of the calculation of N_{agg} from $[Q]_m/[M]$ have been reported elsewhere.[18]

e. Quasielastic Light Scattering (QELS). The apparent hydrodynamic radius (R_h) and the distribution of the relaxation times were measured with an Otsuka Electronics Photal DLS-7000 light scattering spectrometer equipped with a 60 mW Ar laser operating at $\lambda = 488$ nm. Data were collected using an ALV-5000 wide-band multi-τ digital autocorrelator. All measurements were performed at 25 °C. The micelle R_h and the distributions of relaxation times were measured as a function of the polymer concentration and scattering angle. Sample solutions were filtered prior to measurements using a 0.45 μm pore size disposable membrane filter. All the solutions were prepared in 0.1 M NaCl. To obtain the relaxation time distribution, $\tau A(\tau)$, the inverse Laplace transform (ILT) analysis was performed by conforming the REPES algorithm.[32,33] The probability of reject was set to 0.5.

$$g^{(1)}(t) = \int \tau A(\tau) \exp(-t/\tau)\, \mathrm{d} \ln \tau \quad (3)$$

Here, τ is the relaxation time and $g^{(1)}(t)$ is the normalized autocorrelation function. The relaxation time distributions are given as a $\tau A(\tau)$ vs log τ profile with an equal area. Diffusion coefficients, D, are calculated from $D = (\Gamma/q^2)_{q\to 0}$, where Γ is the relaxation rate and q is the magnitude of scattering vector expressed as $q = (4\pi n/\lambda) \sin(q/2)$ where n is the index of refraction of the solution. Diffusion coefficients obtained from QELS measurements depend on the polymer concentration.[34,35] As the polymer concentration is increased, the diffusion coefficient tends to deviate from the diffusion coefficient for a polymer chain completely isolated from others. This deviation arises from hydrodynamic and thermodynamic interactions among interacting polymers. Thus, values of R_h calculated using the Einstein−Stokes equation, $R_h = k_B T/6\pi\eta D$, where k_B is the Boltzmann constant, T is the absolute temperature, and η is the solvent viscosity, are "apparent" hydrodynamic radii.[34,35] The details of the QELS measurement and data analysis have been reported in earlier papers.[32−37]

Results

Characterization of Copolymers. A number of macromonomers have so far been developed and employed for designing a variety of graft copolymers with well-defined structures.[38,39] Among others, various PEO-based macromonomers have been synthesized, and their reactivities and the properties of their polymers have been investigated.[40,41] A macromonomer containing an $(CH_2CH_2O)_n$ chain as a spacer between a polymerizable moiety at one end and a terminal hydrophobe at the other end is employed for preparation of hydrophobically associative thickeners (AT polymers) and their model polymers by copolymerizing with a water-soluble polymer such as acrylamide and (meth)acrylic acid.[42−46]

The contents of the associative comonomers in AT copolymers are normally very low (frequently lower than 2 mol %). In the present study, however, the level of the macromonomer (DE25MA) incorporation is much higher (i.e., up to 30 mol %) because we are interested the self-organization behavior of the polymer due to micelle formation of polymer-bound surfactant moieties.

Copolymerizations of water-soluble monomers and surfactant macromonomers can be carried out in aqueous media in the presence or absence of nonpolymerizable surfactants.[15a,42−44,47] In "micelle" or "emulsion" polymerization, copolymers with a blocky distribution of the surfactant comonomer are likely to be formed.[47−49] To obtain copolymers with random distributions of the two monomer units, we employed homogeneous solution polymerization using DMF as a solvent that can dissolve the two monomers as well as the copolymers yielded.

Figure 1a,b shows ^{1}H NMR spectra of the macromonomer (DE25MA) and an AMPS−DE25MA copolymer prepared with a DE25MA/AMPS mole ratio of 1/9 in the monomer feed. On the basis of the ratio of the area intensities of resonance peaks around 1.0 and 3.5 ppm due to the methyl and methylene protons in the DE25MA and AMPS units, respectively (Figure 1b), the content of DE25MA (f_{DE25}) in the copolymer was estimated to be about 10 mol %, f_{DE25} being practically the same as that in the monomer feed. The values of f_{DE25} for all the copolymers employed in the present study were also estimated in the same manner (Table 1). We also synthesized AMPS−DE25MA copolymers with f_{DE25} > 30 mol %, but these copolymers with higher contents of DE25MA were found to be insoluble in water.

The molecular weights of the copolymers were estimated by GPC calibrated with standard poly(ethylene glycol) (PEO) samples, using methanol containing 0.10 M $LiClO_4$ as an eluent (Table 1). In a separate study, M_w obtained from SLS measurements in methanol

Table 1. Characteristics of the Copolymers

f_{DE25}[a] (mol %)	M_w[b] (10^4)	M_w/M_n[b]	no. of $C_{12}E_{25}$ groups per polymer chain	cmc[c] (g/L)	K_v[d]
10	7.0	3.0	7	0.006	1.1×10^5
15	6.9	1.9	13	0.018	1.0×10^5
20	7.6	2.9	15	0.021	1.1×10^5
30	8.3	2.8	16	0.024	1.2×10^5

[a] Mole percent content of DE25MA in the copolymer determined by ^{1}H NMR in D_2O. [b] Determined by GPC using a 0.1 M $LiClO_4$ methanol solution as an eluent. Standard poly(ethylene oxide) samples were used for the calibration of the molecular weight. [c] Determined from steady-state fluorescence excitation spectra of pyrene probes (see text). [d] Partition coefficient for solubilization of pyrene (see text).

containing 0.10 M $LiClO_4$ was found to be almost the same as the value estimated by GPC. Since we needed to know the number-average molecular weight (M_n) for the calculation of the number of $C_{12}E_{25}$ groups per polymer chain, we used GPC for a rough estimation of M_n. The weight-average molecular weight shows a tendency to increase with increasing f_{DE25}, the molecular weight distributions (M_w/M_n) ranging from 1.9 to 3.1. On the basis of the DE25MA content and the molecular weight, the number of the DE25MA units per polymer chain can be roughly calculated for each copolymer as listed in Table 1.

Hydrophobic Microdomains Formed by Dodecyl Groups. Molecular pyrene is often used as a fluorescence probe for characterization of molecular assemblies.[28,29,44,45,50−54] It is well-established that the steady-state fluorescence spectra and fluorescence lifetime of pyrene provide information about immediate environments for the probe.[51]

Figure 2a shows the steady-state fluorescence spectra of pyrene probes dissolved in 0.1 M NaCl aqueous solutions in the presence of varying concentrations of the copolymers with $f_{DE25} = 20$ mol %. Pyrene is soluble in water at room temperature up to 7×10^{-7} M.[50a,53] In the presence of the polymer, pyrene molecules are partitioned between the polymer phase and the bulk water phase, thus the solubility of pyrene increasing in proportion to the amount of polymer in solution. In the fluorescence measurements for Figure 2, a lower concentration of pyrene (1×10^{-7} M) was employed to ensure complete solubilization of the probe molecules in hydrophobic microdomains formed by polymer-bound $C_{12}E_{25}$ groups. As the polymer concentration (C_p) is increased, starting from 6.10×10^{-3} g/L, an excimer emission starts to occur at $C_p = (1-2) \times 10^{-2}$ g/L. The intensity of the excimer emission (I_E) relative to the monomer emission (I_M) increases with increasing C_p, the I_E/I_M ratio reaching a maximum at C_p = ca. 0.1 g/L, and then decreases with a further increase in C_p. The excimer emission is completely absent at $C_p > 1.56$ g/L. As will be discussed more in detail in a later subsection, the excimer formation has an effect on the decay of monomeric fluorescence of pyrene solubilized in the hydrophobic microdomains. When $C_p < 1.56$ g/L, fluorescence decay curves contain a fast decay component due to quenching of monomeric pyrene fluorescence, arising from the excimer formation. When $C_p > 1.56$ g/L, however, the decays are completely single-exponential with a long lifetime on the order of 380 ns typical of pyrene existing in hydrophobic phases.

These observations indicate that polymer-bound $C_{12}E_{25}$ residues form hydrophobic microdomains by association of dodecyl groups and that some microdomains solubilize two or more pyrene probes when the polymer concentration is low, giving rise to excimer formation within the microdomain. As C_p is increased, the number of the hydrophobic microdomains increases, and pyrene molecules are distributed over the microdomains, thus decreasing the probability of excimer formation. At $C_p > 1.56$ g/L, all the pyrene probes are isolated from others, leading to completely monomeric fluorescence emission.

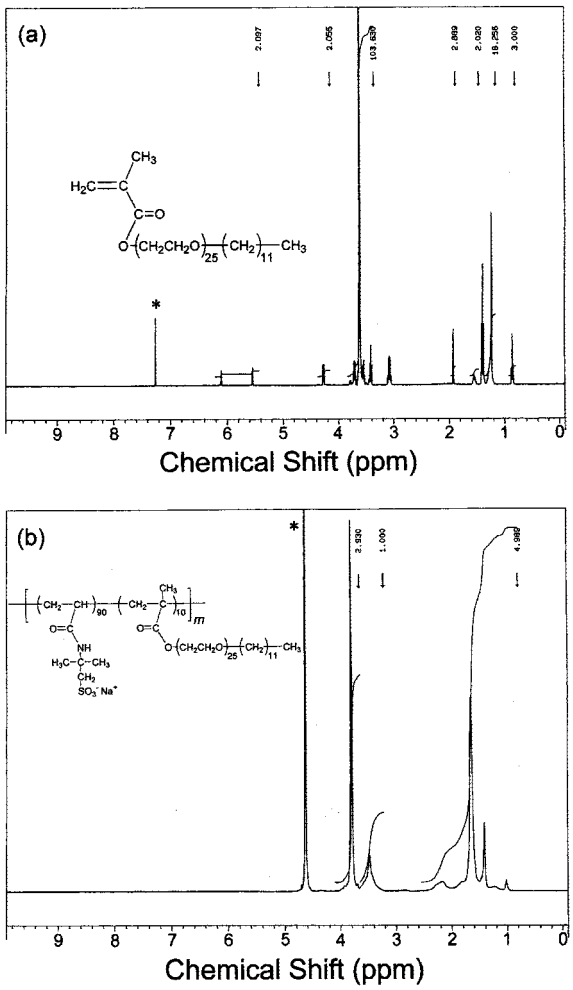

Figure 1. The 400 MHz ^{1}H NMR spectra for DE25MA measured in $CDCl_3$ (1.0 mg/mL) at 30 °C (a) and the copolymer with $f_{DE25} = 10$ mol % measured in D_2O (10 mg/mL) at 60 °C (b).

It is to be noted that the C_p value for the onset of an increase in the I_E/I_M ratio depends on f_{DE25}, the copolymers with larger f_{DE25} exhibiting higher C_p for the onset of the increase in the I_E/I_M ratio. These phenomena will be discussed in the following subsection in connection with the results of critical micelle concentration (cmc).

The intensity of the symmetry-forbidden first vibronic band (I_1), relative to that of the third vibronic band (I_3), in pyrene fluorescence spectra is known to be sensitive to microenvironmental polarity, the I_3/I_1 ratio increasing with decreasing the micropolarity.[51,52] As C_p is increased, there is a tendency that the I_3/I_1 ratio increases (Figure 2a), indicative of solubilization of pyrene probes in hydrophobic microdomains formed by polymer-bound $C_{12}E_{25}$.

Figure 2b shows excitation spectra corresponding to the fluorescence emission spectra in Figure 2a. The excitation spectra were monitored at the pyrene mono-

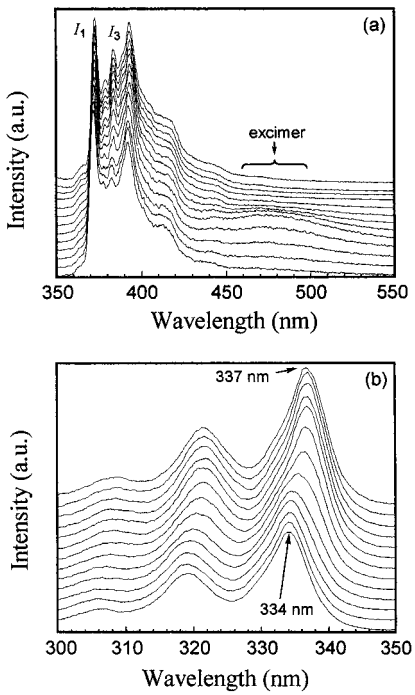

Figure 2. Steady-state fluorescence emission spectra excited at 338 nm (a) and excitation spectra monitored at 338 nm (b) for pyrene in 0.1 M NaCl aqueous solution in the presence of varying concentrations of the copolymer with $f_{DE25} = 20$ mol %. Polymer concentration (from top to bottom); 25.0, 12.5, 6.25, 3.13, 1.56, 0.781, 0.391, 0.195, 0.0977, 0.0488. 0.0244, 0.0122, and 0.00610 g/L. [pyrene] = 1.0×10^{-7} M.

mer fluorescence band at 372 nm. It is known that the pyrene 0−0 absorption band at 334 nm in water shifts toward longer wavelengths when pyrene is solubilized in hydrophobic phases in micelles.[29,55] Given the fact that all pyrene probes are completely solubilized at $C_p > 1.56$ g/L, we can conclude from Figure 2b that the 0−0 absorption band for pyrene solubilized in the hydrophobic microdomains formed by the polymer-bound $C_{12}E_{25}$ shifts to 337 nm. In the C_p region from 6.10×10^{-2} to 7.81×10^{-1} g/L, there is a tendency that the 0−0 absorption band shifts toward longer wavelengths as C_p is increased, indicating that an increasing number of pyrene probes are solubilized in the hydrophobic microdomains with increasing C_p.

Apparent Critical Micelle Concentration (cmc) for Polymer-Bound $C_{12}E_{25}$. The hydrophobic microdomains formed by the polymer-bound $C_{12}E_{25}$ may be viewed as a polymer micelle. In the micelle of the copolymers investigated in this study, the hydrophobic core, consisting of dodecyl groups, is connected polyAMPS chains via long and flexible PEO spacers. The formation of such polymer micelles may occur at a certain critical polymer concentration as in the case of ordinary surfactant micelles.

In Figure 3a, the I_3/I_1 ratios for the copolymers with varying f_{DE25} are plotted against C_p. At the lowest C_p (ca. 10^{-3} g/L), the I_3/I_1 ratios for all the copolymers are in the neighborhood of 0.6, which is practically the same as that for molecular pyrene in water.[51] As C_p is increased, the I_3/I_1 ratio starts to increase significantly at a certain C_p value for a given copolymer. In the case of $f_{DE25} = 10$ mol %, the I_3/I_1 ratio commences to increase at $C_p \sim 6 \times 10^{-3}$ g/L, reaching a constant value of $I_3/I_1 \approx 0.80$ at $C_p \sim 10^{-1}$ g/L. As f_{DE25} is increased, C_p for the onset of the increase in the I_3/I_1 ratio increases. These

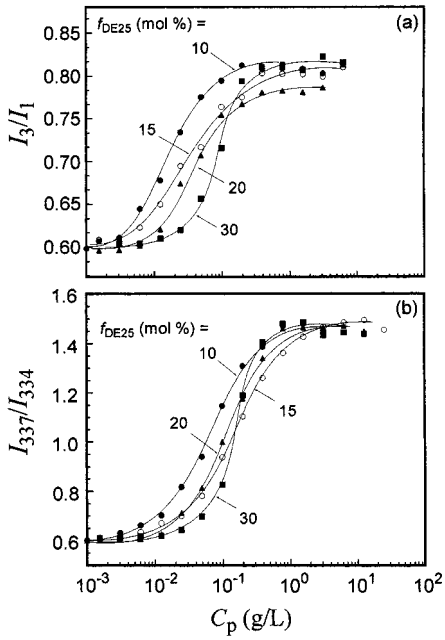

Figure 3. Plots of the I_3/I_1 ratio (a) and the I_{337}/I_{334} ratio (b) as a function of the polymer concentration for the copolymers with varying f_{DE25}.

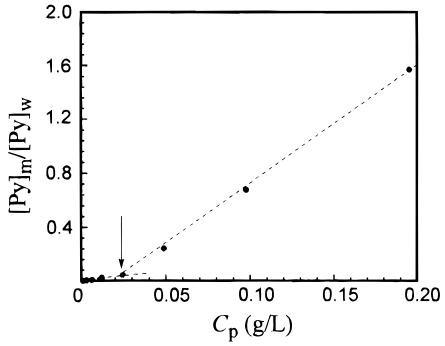

Figure 4. Plot of $[Py]_m/[Py]_w$ estimated from the I_{337}/I_{334} ratio against the polymer concentration for the copolymer with $f_{DE25} = 20$ mol %. An apparent cmc is indicated by an arrow.

results indicate that micelle formation commences to occur at a specific concentration of the polymer.

We attempted to estimate an apparent cmc for the copolymers using excitation spectra, as reported by Wilhelm et al.[29] The ratios of the intensities at 337 nm relative to those at 334 nm (I_{337}/I_{334}) for the four copolymers with varying f_{DE25} are plotted against C_p in Figure 3b. Upon an increase in C_p, the I_{337}/I_{334} ratio exhibits a significant increase at a certain C_p value. On the basis of the data in Figure 3b, we calculated the concentrations of pyrene in the micellar phase ($[Py]_m$) and in the bulk water phase ($[Py]_w$) according to the method reported previously,[18,29,55] and the ratio of $[Py]_m/[Py]_w$ is plotted as a function of C_p in Figure 4. Since the AMPS−DE25MA copolymers consist of a large number of surfactant moieties along the polymer chain, hydrophobic microdomains should be formed via intrapolymer associations even at very low C_p. As can be seen from Figure 4, with increasing C_p, the $[Py]_m/[Py]_w$ ratio increases gradually in a low C_p region ($C_p < 0.03$ g/L) and then increases more significantly in a higher C_p region ($C_p > 0.03$ g/L). The gradual increase in the low C_p regime corresponds to the increased partition of pyrene probes in the hydrophobic microdomains formed via intrapolymer associations. On the other hand, the

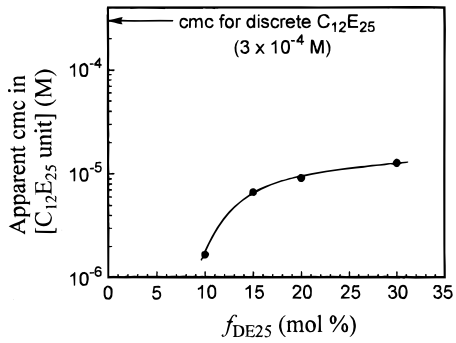

Figure 5. Plots of apparent cmc in terms of the molar concentration of the $C_{12}E_{25}$ unit as a function of f_{DE25}.

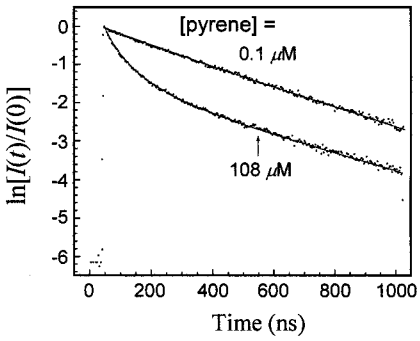

Figure 6. Comparison of fluorescence decays at different concentrations of pyrene solubilized in the presence of the copolymer with f_{DE25} = 20 mol % in 0.1 M NaCl aqueous solution. C_p = 6.25 g/L.

onset of the significant increase in the $[Py]_m/[Py]_w$ ratio corresponds to the onset of micelle formation via interpolymer associations. Thus, an apparent cmc can be estimated from the break in the plot in Figure 4. From the intercept of the sloping lines on the abscissa, apparent cmc values are estimated as listed in Table 1. The partition coefficients (K_v) for pyrene solubilization in micelles formed from the four copolymers were estimated from the slope of the linear line at C_p > cmc in Figure 4, and the results are listed in Table 1. The details of the determination of apparent cmc and K_v were reported in earlier papers.[18,29,55] The value of apparent cmc depends on f_{DE25}. For the copolymer with f_{DE25} = 10 mol %, the cmc value is on the order of 10^{-3} g/L, whereas the cmc increases with an increase in f_{DE25}. Figure 5 shows the plot of the apparent cmc, represented as the molar concentration of the $C_{12}E_{25}$ unit in the copolymer, against f_{DE25}. We determined the cmc for discrete $C_{12}E_{25}$ surfactant molecules in 0.1 M NaCl aqueous solution to be about 3.0×10^{-4} M, using the same technique based on the excitation spectra of solubilized pyrene probes. The apparent cmc values for the copolymers were found to be smaller than the cmc for the corresponding discrete $C_{12}E_{25}$ surfactant by more than an order of magnitude. The increase in the apparent cmc on going from f_{DE25} = 10 to 20 mol % is not well understood.

The K_v values were found to be fairly constant (1.0×10^5–1.2×10^5) for the four copolymers (Table 1), a slightly smaller than the K_v value for the discrete $C_{12}E_{25}$ (1.7×10^5) determined in the present study using the same method. These K_v values for the copolymers are almost the same as a reported value for sodium dodecyl sulfate micelles (1.2×10^5).[29,56]

Aggregation Number (N_{agg}) of Polymer-Bound $C_{12}E_{25}$. The aggregation number N_{agg} of polymer hydrophobes is one of the important parameters to characterize polymer micelles. Various experimental methods for the determination of N_{agg} have been reported.[54,57] In the present study, we determined N_{agg} of dodecyl groups in the copolymers employing a fluorescence technique based on the excimer formation of pyrene probes solubilized in the hydrophobic microdomains of the polymers.[30,31] For the calculation of N_{agg}, we assumed that all pyrene probes were randomly distributed over the hydrophobic microdomains according to a Poisson distribution. Figure 6 shows an example of fluorescence decay data for the copolymer with f_{DE25} = 20 mol % at C_p = 6.25 g/L in a 0.10 M NaCl aqueous solution containing 108 μM pyrene. For comparison, a fluorescence decay for a low concentration of solubilized pyrene (1×10^{-7} M) at the same polymer concentration is also presented in Figure 6. When the concentration of solubilized pyrene is very low such that each hydrophobic microdomain contains much less than one pyrene molecule on average, no excimer is formed, exhibiting a single-exponential decay. As the pyrene concentration is increased, probability of finding two pyrene molecules in the same microdomain increases. If two or more pyrene molecules are solubilized in the same hydrophobic microdomain, excimer may be formed within the same microdomain, yielding to a fast decay component in the decay of monomeric pyrene fluorescence (Figure 6). Kinetic models for the quenching of pyrene monomeric fluorescence in the micelle due to excimer formation have been well-documented by Infelta et al.,[30a,c] Tachiya,[30b,d] and others.[31,58] A simple model is expressed by the Infelta–Tachiya equation (eqs 1 and 2) where distributions of fluorophores and quenchers over the micelles obey a Poisson distribution. Assuming this simple kinetic model, we attempted to fit fluorescence decay data to eq 1 and found all the decay data were able to best fit with χ^2 ranging from 1.10 to 1.31. We performed this experiment at several different concentrations of polymer and pyrene for each copolymer with different f_{DE25}.

Table 2 lists parameters A_2, A_3, and A_4 obtained from the best-fit of the fluorescence decay data to eqs 1 and 2. The average number of pyrene molecules in a micelle, n_Q, can be calculated from these parameters as

$$n_Q = (A_3A_4 + A_2 - k_0)^2/A_3A_4^2 \qquad (4)$$

From the n_Q value thus estimated, the aggregation number of hydrophobes in a hydrophobic microdomain can be calculated.[18] To estimate the n_Q value, τ_0, measured for concentrated polymer solutions with very low amounts of pyrene, should be measured. Fluorescence decay data for 1.0×10^{-7} M pyrene at C_p = 12.5 g/L were best-fitted to a single-exponential function, and τ_0 values were found to be about 380 ns for all the copolymers independent of f_{DE25}. As can be seen in Table 2, however, A_2^{-1} values obtained in a high C_p region for the copolymers with f_{DE25} = 15, 20, and 30 mol % are larger than the τ_0 values (ca. 380 ns). On the other hand, A_2^{-1} values in a low C_p region are slightly smaller than the τ_0 value, and the A_2^{-1} value slightly decreases with decreasing C_p. This may simply mean that the exit rate constant (k^-) for pyrene molecules from a micelle increases with a decrease in C_p. The reason that A_2^{-1} values are larger than the τ_0 value is not well-understood, but this observation may suggest that the

Table 2. Fitting Parameters for Eq 1 and Aggregation Numbers of Dodecyl Groups in the Hydrophobic Microdomain

f_{DE25} (mol %)	C_p (g/L)	[pyrene][a] (μM)	A_3	$10^{-6}A_4$ (s^{-1})	A_2^{-1} (ns)	χ^2	N_{agg}
10	6.25	54.7	2.08	14.1	381	1.21	69
	3.13	26.9	1.91	14.2	382	1.10	66
	1.56	6.87	1.02	13.8	383	1.10	68
	0.781	3.18	0.94	14.0	384	1.12	67
	0.391	1.74	1.04	14.2	383	1.23	66
	0.195	0.890	1.08	14.0	381	1.21	64
15	12.5	162	2.14	13.9	387	1.22	64
	6.25	80.9	2.10	13.9	386	1.18	63
	3.13	42.8	2.27	14.2	380	1.28	62
	1.56	20.3	2.14	14.3	381	1.31	61
	0.781	9.43	2.09	14.2	378	1.30	62
	0.391	4.32	1.89	14.3	378	1.29	61
	0.195	2.32	1.92	14.1	379	1.31	59
	0.0977	1.09	1.89	14.2	378	1.33	61
20	12.5	108	1.11	14.2	402	1.10	57
	6.25	57.4	1.17	14.3	395	1.21	56
	3.13	27.0	1.19	13.9	396	1.27	57
	1.56	15.2	1.24	13.9	387	1.13	56
	1.23	10.7	1.23	14.2	379	1.10	57
	0.617	5.71	1.18	14.3	379	1.10	56
	0.359	2.97	1.21	14.2	377	1.24	58
	0.179	1.42	1.17	14.3	378	1.28	58
30	12.5	342	2.53	13.4	418	1.13	50
	6.25	162	2.51	14.2	397	1.21	51
	3.13	80.3	2.53	14.1	382	1.16	52
	1.56	41.2	2.50	14.2	381	1.16	51
	0.781	20.9	2.61	14.3	379	1.17	52
	0.391	10.1	2.57	14.5	377	1.18	53
	0.195	4.20	2.31	14.1	376	1.25	54
	0.0977	2.10	2.19	14.4	377	1.30	53

[a] Concentrations were calculated from the absorbance at 338 nm using $\epsilon_{338} = 37\,000\ M^{-1}\ cm^{-1}$.[28]

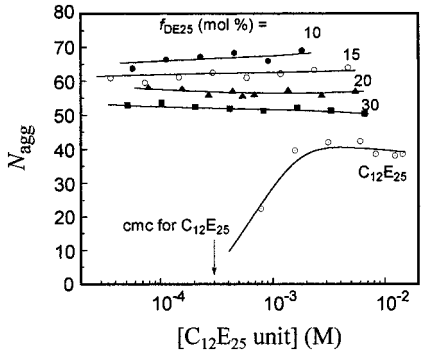

Figure 7. Plots of N_{agg} values against the molar concentration of the $C_{12}E_{25}$ unit for the polymers with varying f_{DE25} in 0.1 M NaCl aqueous solutions. N_{agg} values for the discrete $C_{12}E_{25}$ surfactant are also plotted.

interior of the micelles is more protected from its surroundings at higher polymer concentrations.

N_{agg} values thus estimated are plotted in Figure 7 as a function of the molar concentration of $C_{12}E_{25}$ residues converted from C_p for the copolymers with varying f_{DE25}. In Figure 7, values of N_{agg} for the discrete $C_{12}E_{25}$ molecule in 0.1 M NaCl aqueous solution are also plotted against its concentration. These values were determined using the same fluorescence method in this study and found to be virtually the same as a value for $C_{12}E_{23}$ ($N_{agg} = 40$) reported in the literature.[59] As can be seen from Figure 7, N_{agg} values for the copolymers are larger by 10−30 than those for discrete $C_{12}E_{25}$ at concentrations well above its cmc (3×10^{-4} M), and the N_{agg} value decreases with increasing f_{DE25}.

Hydrodynamic Size of the Polymer Micelles. Figure 8 compares the relaxation time distributions in

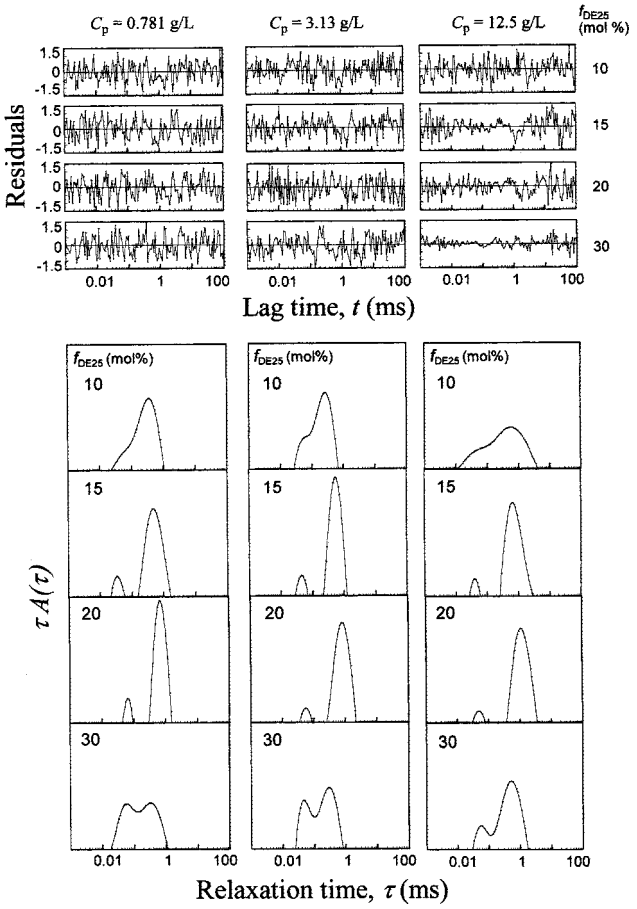

Figure 8. Relaxation time distributions at $\theta = 90°$ for the copolymers with varying f_{DE25} at varying polymer concentrations. Residuals in the computation of the corresponding relaxation time distributions are identical.

QELS observed at a scattering angle of 90° for the copolymers with varying f_{DE25} at three polymer concentrations in 0.1 M NaCl aqueous solutions. All the four polymers show bimodal distributions with fast and slow relaxation modes in the C_p range of 0.781−12.5 g/L. In the case of the copolymers with $f_{DE25} = 15$ and 20 mol %, both the fast and slow mode distributions are narrow enough to yield well-separated two peaks, whereas those for $f_{DE25} = 10$ and 30 mol % are so broad that the two distributions overlap. For the copolymers with $f_{DE25} = 10$ and 15 mol % the distribution profiles are practically independent of C_p within the C_p range studied. On the other hand, for $f_{DE25} = 20$ and 30 mol % the fast mode peak decreases, relative to the slow mode peak, with an increase in C_p. This is particularly so in the case of $f_{DE25} = 30$ mol %. To identify the significance of the fast mode, since the REPES algorithm often returns noisy fast modes of no real significance,[32,33] the residuals for each grid point returned from the program for all the data were carefully checked. The residual data corresponding to each relaxation time distribution are shown in Figure 8. These results confirm that all the fast mode peaks are not artificial ones. To check the significance of the fast mode peaks, we performed two-exponential fitting for all the data, which is available for the ALV software. The individual results of the two-exponential fitting for all the data were found to be consistent with the results of REPES.

Since the copolymers with $f_{DE25} = 15$ and 20 mol % show well-separated two distribution peaks, we can determine apparent hydrodynamic radii (R_h) corre-

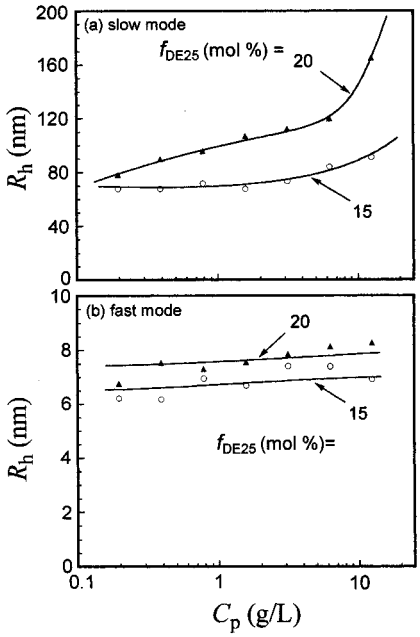

Figure 9. Relationship between R_h and the polymer concentration.

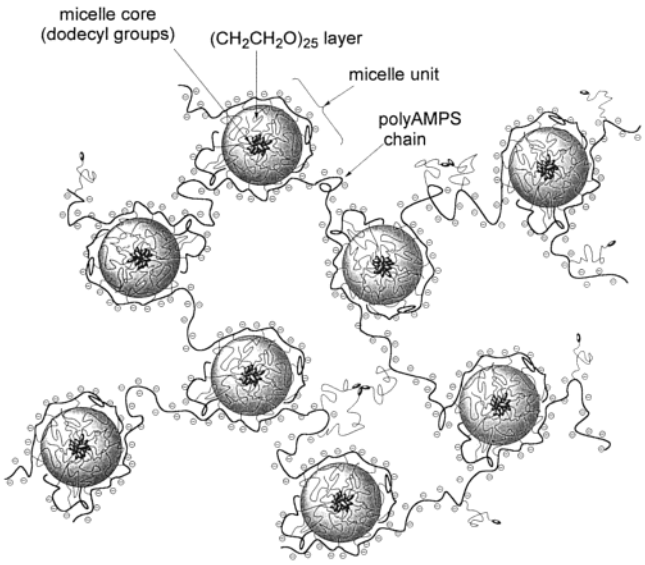

Figure 10. A hypothetical model for bridged multipolymer micelles.

sponding to the fast and slow relaxation modes. To this end, we measured relaxation time distributions for the two polymers at several different scattering angles and plotted the relaxation rates (Γ) (i.e., the reciprocal of the relaxation time) for the fast and slow modes as a function of the square of the scattering vector (q^2). The plots for the two polymers in the C_p range of 0.195−12.5 g/L yielded straight lines passing through the origin (data not shown). These results indicate that both the fast and slow relaxation modes are due to translational diffusion of scatterers. From the diffusion coefficients estimated from the slope of the $\Gamma-q^2$ plot, R_h values corresponding to the fast and slow relaxation modes were calculated using the Einstein−Stokes relation. In Figure 9, R_h values thus estimated for the slow relaxation mode are plotted against C_p. As C_p is increased from 0.195 to 12.5 g/L, R_h values for the copolymers with f_{DE25} = 15 and 20 mol % increase from 68 to 90 nm and from 78 to 165 nm, respectively. The hydrodynamic size for f_{DE25} = 20 mol % is larger than that for f_{DE25} = 15 mol % in the whole range of C_p investigated, and this is more so at higher C_p. In the case of f_{DE25} = 20 mol %, R_h increases more significantly at C_p > 6.25 g/L.

Values of R_h corresponding to the fast relaxation mode for the copolymers with f_{DE25} = 15 and 20 mol % were found to be 6−8 nm over the C_p range of 0.195−12.5 g/L and independent of C_p. This fast mode component may be due to either a "unimeric" micelle (a micelle formed by a single polymer chain) or an "oligomeric" micelle (a micelle formed by a small number of polymer chains), but so far we have not been able to confirm which is the case.

We estimated R_h for micelles formed from discrete $C_{12}E_{25}$ surfactants to be 4−5 nm in 0.1 M NaCl at surfactant concentrations well above the cmc. The hydrodynamic sizes for the slow mode component for the copolymers with f_{DE25} = 15 and 20 mol % are more than 1 order of magnitude larger than that for the discrete micelle of $C_{12}E_{25}$ even at the lowest C_p (i.e., 0.195 g/L). On the other hand, the values of N_{agg} for these copolymers are larger than that for the discrete $C_{12}E_{25}$ micelle by less than twice. From the molecular weight and f_{DE25}, the mean number of dodecyl groups per polymer chain can be roughly calculated to be 7, 13, 15, and 16 for the copolymers with f_{DE25} = 10, 15, 20, and 30 mol %, respectively (Table 1). If we assume that one polymer micelle has only one hydrophobic domain (i.e., a unicore micelle), the polymer aggregation number can be estimated roughly to be about 10, 5, 4, and 3 for the copolymers with f_{DE25} = 10, 15, 20, and 30 mol %, respectively. Therefore, it is obvious that the slow mode component in Figure 8 represents a polymer aggregate which includes a number of micelle units formed by polymer-bound $C_{12}E_{25}$ groups.

It is to be noted here that, in the case of the copolymers with f_{DE25} = 10 and 30 mol %, R_h values, roughly estimated for their slow modes, were found to range from 35 to 70 nm over the C_p range investigated, slightly smaller than those for the copolymers with f_{DE25} = 15 and 20 mol %. Thus, we can conclude that these slow modes for f_{DE25} = 10 and 30 mol % are also due to a similar type of the polymer aggregate found for f_{DE25} = 15 and 20 mol %.

Discussion

On the basis of the experimental results described above, we have come up with a hypothetical model for an associative structure of AMPS−DE25MA copolymers, as illustrated in Figure 10. The polymer-bound $C_{12}E_{25}$ moieties form micelle units whose core size (i.e., N_{agg}) is somewhat similar to that of the corresponding discrete $C_{12}E_{25}$ micelle, i.e., $N_{agg} \approx 50-70$ for the polymer-bound micelle whereas $N_{agg} \approx 40$ for the discrete micelle (Figure 7). The micelle unit is formed from association of the $C_{12}E_{25}$ moieties attached on the same and different polymer chains.

In general, the association process in water for polymer-bound hydrophobes follows either a closed or open association model.[60−62] In closed association, an increase in hydrophobe concentration results in an increase in the number of micelles of the same size. In open association, in contrast, the size of hydrophobe aggregates increases with increasing hydrophobe concentration. The results from the data presented in Figure 7 indicate that the formation of the micelle unit follows a closed association mechanism because the

micelle cores conserve their size (i.e., N_{agg}) over a significant range of concentrations of the polymer-bound hydrophobe.

The ability to solubilize pyrene, in terms of the partition coefficient, for the polymer-bound micelle is also similar to that of the discrete micelle, i.e., $K_v = 1.0 \times 10^5 - 1.2 \times 10^5$ for the polymer-bound micelle (Table 1) and $K_v = 1.7 \times 10^5$ for the discrete micelle.

Given the R_h values for associated polymers are more than 1 order of magnitude larger than that for the discrete micelle, it is obvious that the polymer-bound micelle units are bridged by polymer chains, giving rise to a multipolymer cross-linked structure. This micelle bridging occurs when some dodecyl groups on the different polymer chains occupy the same micelle core (Figure 10). The gradual increase in R_h with increasing C_p in a region $C_p <$ ca. 10 g/L (Figure 9) indicates a gradual increase in the extent of micelle bridging or chain cross-linking with increasing C_p. However, the larger increase in R_h for the copolymer with $f_{DE25} = 20$ mol % near 10 g/L is an indication of formation of a macroscopic network made up of bridged micelles in a concentrated regime.

The extent of cross-linking is related to the number of polymer chains that participate in the formation of the same micelle unit. One can think of two extreme cases: (1) all hydrophobes on the same polymer chain occupy the same micelle core, and (2) they occupy completely different micelle cores. In case 1, the polymer association process follows a closed association mechanism. In case 2, the association should follow an open association model and lead to the formation of an infinite network, ending up with gelation. Clearly, these two extreme cases are unrealistic, particularly so is case 2. The distributions of QELS relaxation times for the slow mode are monodisperse with a quite narrow width and symmetrical shape (Figure 8). These observations suggest that the polymer association process is of a closed type in nature. Therefore, it is reasonable to consider that each micelle unit is formed by $C_{12}E_{25}$ groups mostly on the same polymer chain (intrapolymer association), and a rather minor fraction of $C_{12}E_{25}$ groups on the same polymer chain occupy different micelle units (interpolymer association).

For associative thickener (AT) model polymers, where the contents of associative comonomers in the polymer are much lower than those of the present copolymers, it has been reported that the preference of interpolymer association (i.e., the thickening efficiency) depends on the length of the EO spacer in the associative comonomer.[42,43,46b] Hogen-Esch et al.[43] have reported that, in the case of copolymers of acrylamide and an acrylate substituted with a hydrophobe end-capped $(CH_2CH_2O)_i$ group where i ranges from 1 to 3, longer EO spacers are more effective in promoting interpolymer association.[43] However, a maximum effect of promoting interpolymer association seems to be achieved when i is more or less 10 in the case of hydrophobically modified alkali swellable/soluble emulsions (HASE) model polymers consisting of a hydrophobe end-capped $(CH_2CH_2O)_i$ spacer.[46b] Tam et al.[46b] reported that when the length of the EO spacer was increased from $i = 0$ to 10, a great increase in solution viscosity was observed, but when the spacer length was further increased from $i = 10$ to 40, a substantial decrease in viscosity was observed. These observations indicate that, with increasing i from 10 to 40, the probability of forming interpolymer associations is decreased and in turn the probability of forming intrapolymer associations was increased.[46b] Hogen-Esch et al.[43] have discussed two possible causes for "spacer effects": (1) alleviation of an excluded-volume effect on interpolymer hydrophobic association with increased spacer lengths and (2) "decoupling" of motions of the polymer chain and hydrophobes linked to it.[43] For interpolymer association, the excluded-volume effect should be less important for longer spacer lengths. However, due to an observation that the spacer effect is more pronounced in a smaller i region, they consider the decoupling effect is more plausible.[43] Moreover, they discussed a spacer effect on an entropy loss accompanied by association of hydrophobes into hydrophobic aggregates.[43] This process can be regarded as an "ordering" process, and the insertion of long hydrophilic spacers would minimize this loss of entropy through decoupling the motions of the polymer chain and hydrophobe aggregates.[43]

The copolymers in the present study possess much larger numbers of surfactant macromonomer units in the chain compared to these model AT polymers. Therefore, intrapolymer hydrophobic associations are likely to occur in a cooperative fashion even at very low concentrations of the polymer. In this process, the long flexible, hydrophilic spacer would help minimize an entropy loss as a result of the decoupling effect. Furthermore, the intrapolymer excluded-volume effect should be less serious than the interpolymer excluded-volume effect on the formation of hydrophobic aggregates. However, with increasing polymer concentration, micelle cores thus formed may grow in size (i.e., N_{agg}) as a result of interpolymer associations to attain a minimum free energy coming from a maximum positive entropy involved in hydrophobic interaction. This interpolymer hydrophobic association seems to occur cooperatively, thus exhibiting the occurrence of an apparent cmc (Figure 4). This interpolymer association leads to the formation of micelle bridging. At higher C_p in a concentrated regime, more surfactant groups on the same polymer chain occupy different micelle units, thus leading to the formation of larger network structures, as suggested by the results in Figures 8 and 9.

Conclusions

Micellization of random copolymers of AMPS and DE25MA with f_{DE25} ranging from 10 to 30 mol % was characterized by fluorescence and QELS techniques in 0.1 M NaCl aqueous solutions. Pyrene fluorescence excitation and emission spectra suggest that the polymer-bound surfactants undergo hydrophobic association in both intra- and interpolymer fashions to form micelles with an apparent "cmc" for interpolymer micelle formation 10−100 times lower than that for discrete $C_{12}E_{25}$ molecules. Values for N_{agg} of micelle cores were found to be somewhat larger than that for the discrete $C_{12}E_{25}$ and are relatively constant over a significant range of C_p. The slow mode component in QELS data is due to polymer aggregates which include a number of micelle units formed by polymer-bound $C_{12}E_{25}$ groups, R_h ranging from ca. 60 to ca. 170 nm. R_h for discrete $C_{12}E_{25}$ micelle was found to be ca. 5 nm under the same conditions. On the basis of the characterization, a hypothetical micelle model was proposed where micelle units formed from polymer-bound $C_{12}E_{25}$ moieties are bridged by polymer chains yielding a micelle network structure.

Acknowledgment. This work was supported in part by a Grant-in-Aid for Scientific Research No. 10450354 from the Ministry of Education, Science, Sports, and Culture, Japan.

References and Notes

(1) Zang, Y. X.; Da, A. H.; Hogen-Esch, T. E.; Butler, G. B. In *Water Soluble Polymers: Synthesis, Solution Properties and Application*; Shalaby, S. W., McCormick, C. L., Butler, G. B., Eds.; ACS Symposium Series 467; American Chemical Society: Washington, DC, 1991; p 159.

(2) Varadaraj, R.; Branham, K. D.; McCormick, C. L.; Bock, J. In *Macromolecular Complexes in Chemistry and Biology*; Dubin, P., Bock, J., Davis, R. M., Schulz, D. N., Thies, C., Eds.; Springer-Verlag: Berlin, 1994; p 15 and references therein.

(3) Bock, J.; Varadaraj, R.; Schulz, D. N.; Maurer, J. J. In *Macromolecular Complexes in Chemistry and Biology*; Dubin, P., Bock, J., Davis, R. M., Schulz, D. N., Thies, C., Eds.; Springer-Verlag: Berlin, 1994; p 33 and references therein.

(4) Schmolka, I. R. *J. Am. Oil. Chem. Soc.* **1991**, *68*, 206.

(5) Almgren, M.; Bahadur, P.; Jansson, M.; Li, P.; Brown, W.; Bahadur, A. *J. Colloid Interface Sci.* **1991**, *151*, 157.

(6) Malmsten, M.; Lindman, B. *Macromolecules* **1992**, *25*, 5440.

(7) (a)Linse, P.; Björling, M. *Macromolecules* **1991**, *24*, 6700. (b) Linse, P.; Malmsten, M. *Macromolecules* **1992**, *25*, 5434. (c) Linse, P. *J. Phys. Chem.* **1993**, *97*, 13896. (d) Linse, P. *Macromolecules* **1993**, *26*, 4437. (e) Linse, P. *Macromolecules* **1994**, *27*, 2685. (f) Malmsten, M.; Linse, P.; Zhang, K.-W. *Macromolecules* **1993**, *26*, 2905.

(8) Webber, S. E. *Chem. Rev.* **1990**, *90*, 1469.

(9) Glatter, O.; Günther, S.; Schilén, K.; Brown, W. *Macromolecules* **1994**, *27*, 6046.

(10) Hurter, P. N.; Scheutjens, J. M. H. M.; Hatton, A T. *Macromolecules* **1993**, *26*, 5592.

(11) Webber, S. E. *J. Phys. Chem. B* **1998**, *102*, 2618.

(12) McCormick, C. L.; Bock, J.; Schulz, D. N. "Water-Soluble Polymers". In *Encyclopedia of Polymer Science and Engineering*, 2nd ed.; Kroschwitz, J. I., Ed.; John Wiley: New York, 1989; Vol. 11.

(13) Laschewsky, A. *Adv. Polym. Sci.* **1995**, *124*, 1.

(14) Morishima, Y. In *Solvents and Self-Organization of Polymers*; Webber, S. E., Tuzar, D., Munk, P., Eds.; Kluwer Academic Publishers: Dordrecht, The Netherlands, 1996; p 331.

(15) (a) Chang, Y.; McCormick, C. L. *Macromolecules* **1993**, *26*, 6121. (b) McCormick, C. L.; Chang, Y. *Macromolecules* **1994**, *27*, 2151. (c) Kramer, M. C.; Welch, C. G.; Steger, J. R.; McCormick, C. L. *Macromolecules* **1995**, *28*, 5248. (d) Hu, Y.; Kramer, M. C.; Boudreaux, C. J.; McCormick, C. L. *Macromolecules* **1995**, *28*, 7100. (e) Branham, K. D.; Snowden, H. S.; McCormick, C. L. *Macromolecules* **1996**, *29*, 254. (f) Kramer, M. C.; Steger, J. R.; Hu, Y.; McCormick, C. L. *Macromolecules* **1996**, *29*, 1992. (g) Hu, Y.; Smith, G. L.; Richardson, M. F.; McCormick, C. L. *Macromolecules* **1997**, *30*, 3526. (h) Hu, Y.; Armentrout, R. S.; McCormick, C. L. *Macromolecules* **1997**, *30*, 3538.

(16) Morishima, Y.; Nomura, S.; Ikeda, T.; Seki, M.; Kamachi, M. *Macromolecules* **1995**, *28*, 2874.

(17) Yusa, S.; Kamachi, M.; Morishima, Y. *Langmuir* **1998**, *14*, 6059.

(18) Noda, T.; Morishima, Y. *Macromolecules* **1999**, *32*, 4631.

(19) Morishima, Y. *Trends Polym. Sci.* **1994**, *2*, 31.

(20) Morishima, Y.; Tominaga, Y.; Kamachi, M.; Okada, T.; Hirata, Y.; Mataga, N. *J. Phys. Chem.* **1991**, *95*, 6027.

(21) Yamamoto, H.; Mizusaki, M.; Yoda, K.; Morishima, Y. *Macromolecules* **1998**, *31*, 3588.

(22) Morishima, Y. *Prog. Polym. Sci.* **1990**, *15*, 949.

(23) Morishima, Y. *Adv. Polym. Sci.* **1992**, *104*, 51.

(24) Morishima, Y. *Bio-Industry* **1995**, *12*, 20.

(25) Morishima, Y.; Seki, M.; Nomura, S.; Kamachi, M. In *Macroion Characterization: From Dilute Solutions to Complex Fluids*; Schmitz, K. S., Ed.; ACS Symposium Series 548; American Chemical Society: Washington, DC, 1994; p 243.

(26) Morishima, Y. In *Multidimensional Spectroscopy of Polymers: Vibrational, NMR, and Fluorescence Techniques*; Urban, M. W., Provder, T., Eds.; ACS Symposium Series 598; American Chemical Society: Washington, DC, 1995; p 490.

(27) Yamamoto, H.; Morishima, Y. *Macromolecules* **1999**, *32*, 7469.

(28) Vorobyova, O.; Yekta, A.; Winnik, M. A.; Lau, W. *Macromolecules* **1998**, *31*, 8998.

(29) Wilhelm, M.; Zhao, C.-L.; Wang, Y.; Xu, R.; Winnik, M. A.; Mura, J.-L.; Riess, G.; Croucher, M. D. *Macromolecules* **1991**, *24*, 1033.

(30) (a) Infelta, P. P.; Grätzel, M.; Thomas, J. K. *J. Phys. Chem.* **1974**, *78*, 190. (b)Tachiya, M. *Chem. Phys. Lett.* **1975**, *33*, 289. (c) Infelta, P. P. *Chem. Phys. Lett.* **1979**, *61*, 88. (d) Tachiya, M. In *Kinetics of Nonhomogeneous* Processes; Freeman, G. R., Ed.; John Wiley & Sons: New York, 1987; Chapter 11, pp 575−650.

(31) Yekta, A.; Aikawa, M.; Turro, N. J. *Chem. Phys. Lett.* **1979**, *63*, 543.

(32) (a) Jakeš, J. *Czech. J. Phys.* **1988**, *B38*, 1305. (b) Jakeš, J.; Štěpánek, P. *Czech. J. Phys.* **1990**, *B40*, 972. (c) Štěpánek, P. In *Dynamic Light Scattering: The Method and Some Applications*; Brown, W., Ed.; Oxford University Press: New York, 1993; Chapter 4, pp 177−241 and references cited therein.

(33) (a) Nicolai, T.; Brown, W.; Hvidt, S.; Heller, K. *Macromolecules* **1990**, *23*, 5088. (b) Brown, W.; Štěpánek, P. *Macromolecules* **1988**, *21*, 1791. (c) Brown, W.; Nicolai, T.; Hvidt, S.; Štěpánek, P. *Macromolecules* **1990**, *23*, 3, 357.

(34) Selser, J. In *Light Scattering: Principles and development*; Brown, W., Ed.; Oxford University Press: New York, 1996; Chapter 7, pp 232−254 and references therein.

(35) Nicolai, T.; Brown, W. In *Light Scattering: Principles and Development*; Brown, W., Ed.; Oxford University Press: New York, 1996; Chapter 5, pp 166−200 and references therein.

(36) (a) Schätzel, K. In *Dynamic Light Scattering: The Method and Some Applications*; Brown, W., Ed.; Oxford University Press: New York, 1993; Chapter 2, pp 76−148 and references therein. (b) Peters, R. In *Dynamic Light Scattering: The Method and Some Applications*; Brown, W., Ed.; Oxford University Press: New York, 1993; Chapter 3, pp 149−176 and references therein.

(37) Phillies, G. D. J. *Anal. Chem.* **1990**, *62*, 1049A; *J. Chem. Phys.* **1988**, *89*, 91.

(38) Yamashita, Y. *Kobunshi* **1982**, *31*, 988.

(39) Rempp, P. F.; Franta, E. *Adv. Polym. Sci.* **1984**, *58*, 1.

(40) (a) Hertler, W. R. In *Macromolecular Design of Polymeric Materials*; Hatada, K., Kitayama, T., Vogl, O., Eds.; Marcel Dekker: New York, 1997; pp 113−117. (b) Hatada, K.; Kitayama, T. In *Macromolecular Design of Polymeric Materials*; Hatada, K., Kitayama, T., Vogl, O., Eds.; Marcel Dekker: New York, 1997; pp 151−155.

(41) (a) Ito, K.; Tsuchida, H.; Hayashi, A.; Kitano, T.; Yamada, E.; Matsumoto, T. *Polym. J.* **1985**, *17*, 827. (b) Nomura, E.; Ito, K.; Kajiwara, A.; Kamachi, M. *Macromolecules* **1997**, *30*, 2811. (c) Ito, K.; Tanaka, K.; Tanaka, H.; Imai, G.; Kawaguchi, S.; Itsuno, S. *Macromolecules* **1991**, *24*, 2348. (d) Kawaguchi, S.; Yekta, A.; Duhamel, J.; Winnik, M. A.; Ito, K. *J. Phys. Chem.* **1994**, *98*, 7891.

(42) Schultz, D. N.; Kaladas, J. J.; Maurer, J. J.; Bock, J.; Pace, S. J.; Schultz, W. W. *Polymer* **1987**, *28*, 2110.

(43) Hwang, F. S.; Hogen-Esch, T. E. *Macromolecules* **1995**, *28*, 3328.

(44) Kumacheva, E.; Rharbi, Y.; Winnik, M. A.; Guo, L.; Tam, K. C.; Jenkins, R. D. *Langmuir* **1997**, *13*, 182.

(45) Horiuchi, K.; Rharbi, Y.; Spiro, J. G.; Yekta, A.; Winnik, M. A.; Jenkins, R. D.; Bassett, D. R. *Langmuir* **1999**, *15*, 1644.

(46) (a) Tirtaatmadja, V.; Tam, K. C.; Jenkins, R. D. *Macromolecules* **1997**, *30*, 1426, 3271. (b) Tam, K. C.; Farmer, M. L.; Jenkins, R. D.; Bassett, D. R. *J. Polym. Sci., Part B* **1998**, *36*, 2275.

(47) Ezzell, S. A.; Hoyle, C. E.; Greed, D.; McCormick, C. L. *Macromolecules* **1992**, *25*, 1887.

(48) Hill, A.; Candau, F.; Selb, J. *Macromolecules* **1993**, *26*, 4521.

(49) Dowling, K. C.; Thomas, J. K. *Macromolecules* **1990**, *23*, 1059.

(50) (a) Yekta, A.; Xu, B.; Duhamel, J.; Adiwidjaja, H.; Winnik, M. A. *Macromolecules* **1995**, *28*, 956. (b) Xu, B.; Li, L.; Yekta, A.; Masoumi, Z.; Kanagalingam, S.; Winnik, M. A.; Zhang, K.; Macdonald, P. M.; Menchen, S. *Langmuir* **1997**, *13*, 2447. (c) Xu, B.; Zhang, K.; Macdonald, P. M.; Winnik, M. A.; Jenkins, R. D.; Bassett, D. R.; Wolf, D.; Nuyken, O. *Langmuir* **1997**, *13*, 6896.

(51) Kalyanasundaram, K.; Thomas, J. K. *J. Am. Chem. Soc.* **1977**, *99*, 2039.

(52) Nakajima, A. *J. Mol. Spectrosc.* **1976**, *61*, 467.

(53) Zana, R. In *Surfactant Solutions: New Methods of Investigation*; Zana, R., Ed.; Marcel Dekker: New York, 1986; pp 241−294.

(54) *Physico-Chemical Properties of Selected Anionic, Cationic and Nonionic Surfactants*; van Os, N. M., Haak, J. R., Rupert, L. A. M., Eds.; Elsevier Science Publishers B. V.: Dordrecht, The Netherlands, 1993.
(55) Astafieva, I.; Zhong, X. F.; Eisenberg, A. *Macromolecules* **1993**, *26*, 7339.
(56) Almgren, M.; Grieser, F.; Thomas, J. K. *J. Am. Chem. Soc.* **1979**, *101*, 279.
(57) For example: (a) Aniansson, E. A. G.; Wall, S. N.; Almgren, M.; Hoffman, H.; Kielman, I.; Ulbricht, W.; Zana, R.; Lang, J.; Tondre, C. *J. Phys. Chem.* **1976**, *80*, 905. (b) Chang, J. N.; Kaler, E. W. *J. Phys. Chem.* **1985**, *89*, 9. Corti, M.; Degiorgio, V. *J. Phys. Chem.* **1981**, *85*, 711. (c) Hayter, J. B.; Penfold, J. *Colloid Polym. Sci.* **1983**, *261*, 1022. (d) Lianos, P.; Zana, R. *J. Colloid Interface Sci.* **1981**, *84*, 100. (e) Turro, N. J.; Yekta, A. *J. Am. Chem. Soc.* **1978**, *100*, 5951. (f) Croonen, Y.; Geladé, E.; Zegel, van der M.; Auweraer, van der M.; Vandendriessche, H.; Schryver, de F. C.; Almgren M. *J. Phys. Chem.* **1983**, *87*, 1426.
(58) Malliaris, A.; Lang, J.; Sturm, J.; Zana, R. *J. Phys. Chem.* **1987**, *91*, 1475.
(59) Becher, P. *J. Colloid Sci.* **1962**, *17*, 325.
(60) Elias, H. G. *J. Macromol. Sci., Part A* **1973**, *7*, 601.
(61) Halperin, A. *Macromolecules* **1991**, *24*, 1418.
(62) Semenov, A. N.; Joanny, J.-F.; Khokhlov, A. R. *Macromolecules* **1995**, *28*, 1066.

MA991680X